Anisotropic Growth of Oxide Nanocrystals: Insights into the Rutile TiO_2 Phase

Caue Ribeiro,*,† Cristiane Vila,‡ Daniel B. Stroppa,‡ Valmor R. Mastelaro,# Jefferson Bettini,¶ Elson Longo,§ and Edson R. Leite‡

EMBRAPA Instrumentação Agropecuária, Rua XV de Novembro, 1452, 13560-970, CP 741, São Carlos, SP, Brazil, LIEC, Departamento de Química, Universidade Federal de São Carlos, Rod. Washington Luiz, km 235, 13565-905, São Carlos, SP, Brazil, Instituto de Física de São Carlos, Universidade de São Paulo, Av. Trabalhador Sãocarlense 400, 13560-970, São Carlos, SP, Brazil, Laboratório Nacional de Luz Sincroton (LNLS), CP 6192, 13084-971, Campinas, SP, Brazil, and LIEC, Instituto de Química, Universidade Estadual Paulista, Rua Francisco Degni, s/n 14800-900, Araraquara, SP, Brazil

Received: January 3, 2007; In Final Form: February 22, 2007

In this work, we report the synthesis of titanium oxide nanocrystals, especially the rutile TiO_2 phase with nanorod morphology, by a method based on peroxotitanium complex decomposition. The results indicate that the anisotropic morphology reported for rutile TiO_2 nanocrystals is related to the oriented attachment process. Despite the predominance of rutile nanocrystals at longer treatment times, the nanocrystals were obtained also in the anatase type, according to the degradation time adopted. XANES results evidenced the absence of structural correlation between the peroxytitanium complex and phase evolution, and the coexistence of the two phases strongly suggests a correlation of the oriented attachment mechanism and the rutile phase stabilization.

Introduction

Titania, or titanium oxide (TiO_2), is a functional material for which there are several technological applications strongly related to its crystalline structure and nanocrystal size and morphology.[1−6] Each phase of TiO_2 (anatase, brookite, and rutile) displays different physical properties having different functionalities. Thus, from the technological and scientific standpoint, it is important to develop new routes of synthesis whereby the crystalline structure and the size and shape of TiO_2 nanocrystals can be tailored.

The literature contains reports of several studies on the synthesis, phase evolution, and particle morphology of TiO_2 nanocrystals.[7−12] Most of these studies have focused on the anatase TiO_2 phase, while studies on the synthesis and nanocrystal growth mechanism in the rutile TiO_2 phase are less common. Several reports have recently been published on the synthesis of rutile TiO_2 with a variety of particle morphologies.[13−15] Wang et al.[13] reported on the synthesis of rod-like nanocrystals (nanorods) of rutile TiO_2 based on the hydrolysis of $TiCl_4$ in acidic aqueous/alcohol solution. According to these authors, the addition of alcohol is important for the formation of uniform nanorods, although they also found nanorods in acidic water solution. Zhang and Gao[14] and Wu and coauthors,[15] who also reported on the synthesis of rutile TiO_2, stated that the crucial parameter to achieve morphological control over the rutile nanocrystal is the concentration of chloride ions (Cl^-) in the precursor solution.

Despite these recent efforts to synthesize rutile nanorods, the mechanism responsible for the growth process remains unclear. In the present article, we show that the rod-like nanocrystal morphology of the rutile TiO_2 is related to the oriented attachment (OA) nanocrystal growth process, that is, a process involving spontaneous self-organization of adjacent nanocrystals and coalescence.[16−18] In order to achieve this goal, we develop an alternative route of synthesis based on the decomposition of a peroxo complex of titanium (PCT).[19,20] The role of hydrogen peroxide in the synthesis process is basically the formation of a peroxo complex with Ti, evidenced by the yellow color of the solution. This precursor allows one to minimize the presence of ions in the precursor solution, leading to a halogen- and carbon-free process.

Experimental

Rutile TiO_2 was synthesized by hydrothermal treatment of the peroxo complex of a titanium gel solution. PCT gel was prepared from titanium(IV) isopropoxide ($Ti(OCH(CH_3)_2)_4$ 99.999%, Aldrich, U.S.A.) and hydrogen peroxide (H_2O_2 P.A., Mallinckrodt Baker, U.S.A., 30% in volume). In a typical process of synthesis, 2.84 g of titanium isopropoxide was added slowly to an excess quantity of H_2O_2 (11.3 g of a 30 wt % H_2O_2 solution), 10:1 mol % H_2O_2/Ti, under vigorous stirring in an ice bath to prevent H_2O_2 decomposition. A clear brown solution was obtained in this step, with total consumption of the titanium precursor, which characterizes the peroxo complex of Ti formation. The final volume of the solution was then adjusted to 100 mL, using distilled water, and was poured into a round-bottomed flask. In this step, we believe that the peroxo complex of Ti is just formed. The flask was then connected to a reflux apparatus to prevent water evaporation and was allowed to release O_2 produced by the decomposition of excess H_2O_2. The solution was kept refluxing at 80 °C, and a transparent

* To whom correspondence should be addressed. E-mail: caue@cnpdia.embrapa.br.
† EMBRAPA Instrumentação Agropecuária.
‡ Universidade Federal de São Carlos.
# Universidade de São Paulo.
¶ LNLS.
§ Universidade Estadual Paulista.

10.1021/jp070051j CCC: $37.00
Published on Web 03/29/2007

yellow gel was obtained after 15 min. This gel is stable for several weeks. An aliquot of the gel (10 g) was dissolved in water (90 g), and the resulting solution (with pH = 3) was poured into a flask with an autoclavable screw cap. The flask was then placed in a regular laboratory oven and subjected to a constant temperature (95 °C) for several hours, precipitating the TiO_2 nanoparticles by the thermal destabilization of PCT gel. One advantage of the procedure is the control of the precipitation times since they are much larger than those observed in conventional sol−gel hydrolysis,[6,9] allowing a fine tailoring of the precipitated particles.

The titanium K-edge X-ray absorption spectra were collected at the LNLS (National Synchrotron Light Laboratory) facility using the D04B-XAS1 beam line. The LNLS storage ring was operated at 1.36 GeV and 100−160 mA. XAS data were collected at the Ti K-edge (4966 eV) in transmission mode at room temperature using a Si(111) channel-cut monochromator. Ionization chambers were used to detect the incident and the transmitted flux. XANES (X-ray absorption near-edge structure) spectra at the Ti K-edge were recorded for each sample between 4910 and 5100 eV using energy steps of 0.4 eV at the preedge region. To provide good energy reproducibility during the XANES data collection, the energy calibration of the monochromator was checked during the collection of the sample data using a Ti metal foil. For comparison purposes among different samples, all spectra were background removed and normalized using the first EXAFS oscillation as unity.

XRD analysis of the obtained nanoparticles was carried out on a Rigaku, D-Max 2500 instrument, using Cu Kα radiation. The samples were prepared by sonicating the colloids and dropping them on a glass sample holder (at least 55−60 °C) to form a thick film, useful for the XRD measurement. This procedure avoids segregation or sedimentation of the system. The phase concentration was calculated based on the area of (101) anatase and (110) rutile peaks. In this study, the peaks were fitted using a pseudovoigth function in order to calculate the peak area.

The nanocrystal morphology was characterized by scanning transmission electron microscopy (STEM FE−SEM, Zeiss, Supra 35, at 30 kV) and high-resolution transmission electron microscopy (HRTEM, Jeol, 3010, at 300kV). For the STEM/HRTEM study, a drop of the colloidal suspension was deposited on a carbon-covered copper grid for 20 s, followed by drying in air. The particle size distribution was estimated by the measurement of at least 200 particles in the TEM images.

Results and Discussion

Possible correlations of the TiO_2 structure and the peroxo complex of the titanium (PCT) gel structure were mainly investigated by XANES, comparing the spectra from gel and amorphous powder samples (obtained in short treatment times) to crystalline anatase and rutile powders. Figure 1a and b shows the Ti K-edge XANES spectra of PCT gel and TiO_2 amorphous/poorly crystalline powder samples (hydrothermalized for 1 and 6 h). The preedge and postedge region of the TiO_2 gel and amorphous samples are quite similar, indicating that the short-range order does not changes significantly until 6 h of heat treatment.

The preedge region of the XANES spectra of anatase and rutile contains three major features denoted as A1, A3, and B, which are shown in more detail in Figure 1b. The origin of the A3 and B features are attributed to 1s → 3d transitions and assigned to 1s → $2t_{2g}$ and 1s → $3e_g$ transitions in an octahedral field, respectively.[21] The origin of the A1 peak is less clear,

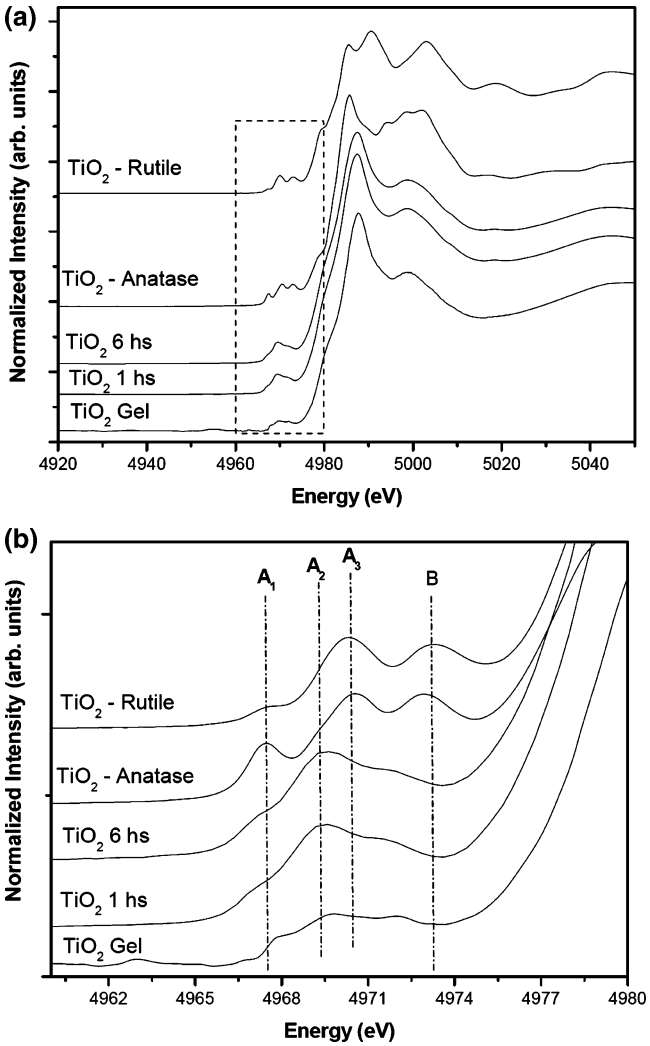

Figure 1. (a) Ti K-edge XANES spectra of the PCT gel and TiO_2 amorphous powder samples obtained by hydrothermal treatment of the PCT gel; also shown for comparison are the spectra of crystalline anatase and rutile powders. The region marked by dotted lines is seen in (b) in better detail.

but it is also believed to be associated with Ti 3d−4p hybridized states.[21]

The additional strong peak A2 observed in the TiO_2 gel and amorphous powder samples has been attributed by different authors to five-coordinate titanium species due to a reduction in the average coordination number of the titanium as the particle surface makes a large contribution.[22,23] An increase in the intensity of the A2 peak of the TiO_2 XANES spectrum from the gel to the amorphous powder has also been observed, which was correlated to an increase in the distortion of the octahedral TiO_6 unit. This result is consistent with the postulated five-coordinate structure proposed by Mühlebach[19] to the precipitated peroxytitanium hydrate, although Schwarzenbach[20] observed the coexistence of the TiO_5− and TiO_6− in solution. The probable structure[19,20] in this case is $[(OH)_2TiO_5Ti]_n$.

Chen and co-workers[21] observed the same behavior in the A2 peak for TiO_2 nanoparticles obtained by $TiCl_4$ hydrolysis, and the authors correlated this behavior to the particle sizes of the samples; as particle size becomes smaller, more Ti atoms are exposed on the surface of the particle experiencing an anisotropic environment where the Ti atom bonds to inner and outer O atoms simultaneously. This anisotropic environment for the surface Ti atoms may be the cause of the possible distortion around Ti atoms from an octahedral TiO_6 unit. It is important

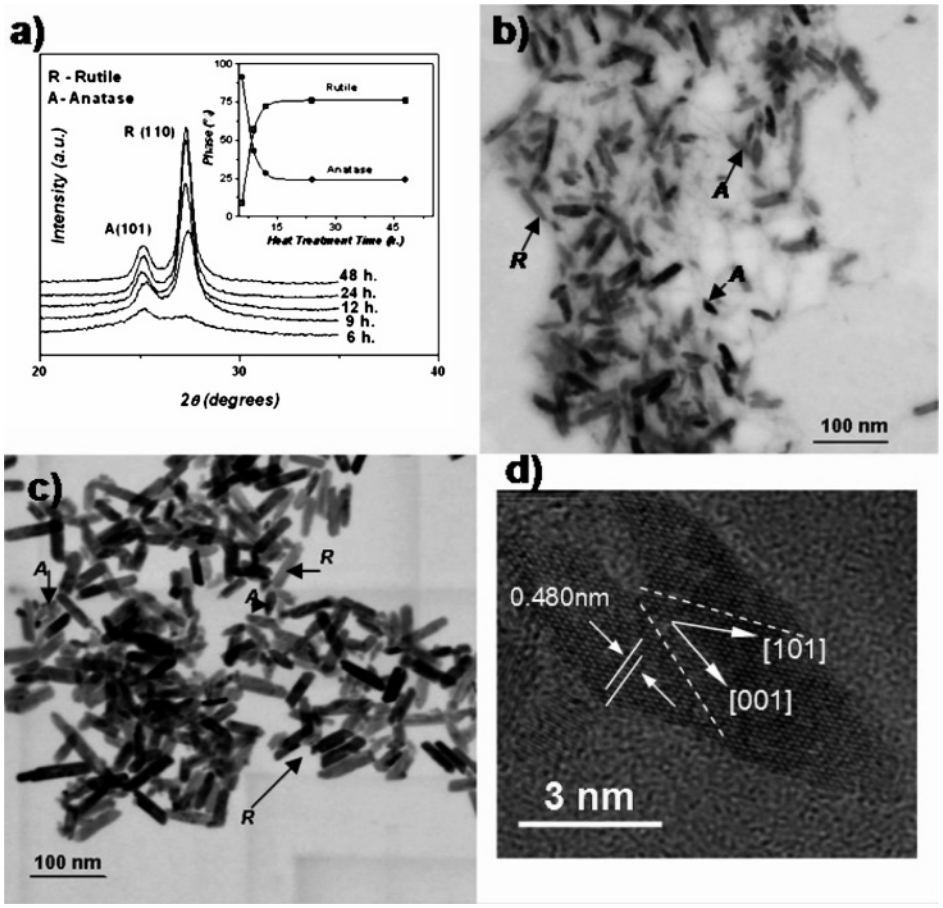

Figure 2. (a) XRD analysis of the PCT gel solution decomposed at 95 °C at different times. Inset shows the phase concentration of the anatase (A) and rutile (R) as a function of decomposition time; (b) low-magnification, bright-field STEM images of the TiO_2 nanocrystal treated for 12 h at 95 °C; (c) 24 h of treatment at 95 °C; (d) HRTEM of the nanocrystals with bipyramid morphology.

to note that both TiO_2 anatase and rutile (references) showed well-defined peaks correlated to six-coordinate titanium species, as expected.

The postedge region of the Ti K-edge XANES spectra of the gel and amorphous powder samples are also quite similar. This region of the XANES spectra are related to multiple scattering contributions due to atoms located at the second coordination shell and further. The presence of large and not-well-defined transitions in this region is characteristic of a relative disordered structure. Especially in PCT gel, this relative disorder is expected since the peroxytitanium structure can be described in several ways, with reported structures with four-, five-, and six-coordinate titanium species, among others.[19,20,24] By these results, we can affirm that the structure of the PCT gel is closer to the amorphous TiO_2 specimen, and the formation of any crystalline phase by the gel decomposition cannot be correlated to "memory" effects of the gel structure. This is an important feature of the system since we can affirm that the phase formation should follow the Ostwald step rule, that is, the gradual crystallization from the metastable to stable phases (i.e., the crystallization path to rutile will necessarily pass through amorphous → anatase → rutile, at least).[25]

A qualitative analysis of the crystallization of the TiO_2 species was done by X-ray diffraction (XRD) analysis of the PCT gel solution decomposed at 95 °C at several times (Figure 2a). The results indicate that anatase TiO_2 is the preferential crystalline phase formed at short treatment times, as expected according the Ostwald step rule. Increasing the treatment time, we found that two TiO_2 phases (anatase and rutile) coexisted and that the volume of the rutile phase increased in detriment to the anatase phase (see inset of Figure 2a). A similar finding was reported by Wu and coauthors[15] who stated that this phase transformation occurs simultaneously with particle growth in a highly acidic medium.

The morphology of the samples was investigated by means of low-magnification, bright-field STEM images of the TiO_2 nanocrystals processed during different treatment times (shown in Figure 2b and c). The figure reveals two types of particle morphologies, nanorods and bipyramid nanoparticles, where the bipyramid nanocrystal is more common in the samples treated for a shorter time. An analysis of lattice images taken by HRTEM (Figure 2d) clearly shows that the bipyramidal nanocrystals present an anatase structure. The rod-like particles can be identified as rutile nanoparticles, being the majority at larger treatment times. It is important to point out that, in several tilts of the sample holder, the HRTEM analysis of the rod-like nanocrystal showed no shape modification, confirming the rod morphology.

Two dimensions can be defined for the nanorod morphology, length (L) and diameter (ϕ). Figure 3 shows the L and ϕ size distribution of the sample prepared at different periods of time. For instance, nanorods with an average $<L> = 39$ nm and an average $<\phi> = 11.6$ nm were obtained for a 12 hour treatment time. For longer treatment times (24 h) at the same decomposition temperature, the $<L>$ measured was 53 nm and the $<\phi>$ was 13.7 nm. The $<L>$ value of the sample treated for 24 h was 1.5 times higher than the $<L>$ value of the sample treated for 12 h, while the $<\phi>$ value of the sample treated for 24 h was 1.2 times higher than the $<\phi>$ value of the sample treated for 12 h. These results suggest a preferential growth in the L

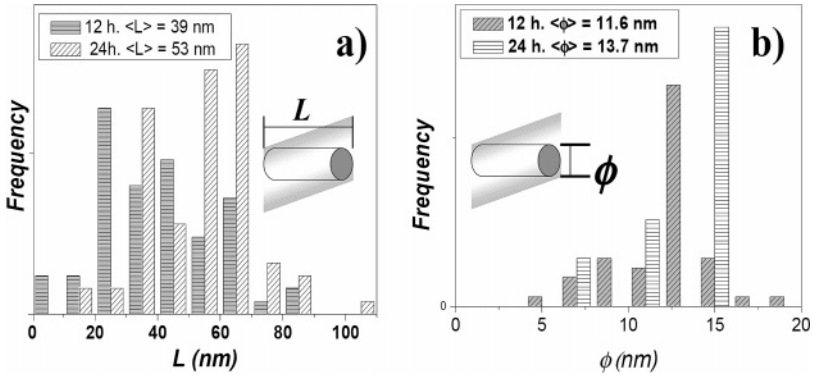

Figure 3. (a) Size distribution of the L dimension of the PCT solution heat-treated for 12 and 24 h. (b) Size distribution of the ϕ dimension for the PCT solution heat-treated for 12 and 24 h (PCT solution decomposition at 95 °C).

dimension. It should be noted that growth and phase transformation occur concomitantly.

HRTEM characterizations were done in order to shed light on the crystal growth mechanism of rutile TiO_2 nanorods. A detailed analysis of the rod-like nanocrystals (obtained after 24 h of hydrothermalization) depicted in Figure 4a and b indicates that the nanorod was composed of several oriented primary particles. A fast Fourier transform (FFT) analysis performed in three different regions of the nanorod (see inset of Figure 4b) confirmed that the primary particles were similarly oriented. Note that the L dimension of the nanorod is related to the [110], indicating a preferential growth in this crystallographic orientation, and the ϕ dimension is related to the [001]. Figure 4c and e provides additional evidence that coalescence occurred when several particles assumed the same orientation, resulting in a single large particle. These figures show reconstructed lattice images of different areas of a nanorod, as indicated in Figure 4b. This kind of image treatment provides a better view of the defects, revealing different degrees of misorientation (indicated by arrows).

The imperfectly oriented attachment may produce different kinds of defects, depending on the rotational relation of one nanocrystal to the others.[16] Figure 4e shows a boundary between two nanoparticles with a perfect orientation. The experimental observations reported before, that is, the aggregation of several nanocrystals with the same crystallographic orientation originating a single nanorod and the presence of defects, are strong evidence that the OA process is the dominant nanocrystal growth mechanism.[16−18] The attachment can be the product of the interaction among anatase nanoparticles or rutile nanoparticles, but at the moment, the distinction is not possible. In this sense, the OA may help the phase transformation since the transformation anatase → rutile is faster in small particles, going to slow rates in larger particles.[26] This aspect can be related to the high growth rates associated to the OA mechanism[27,28] and is also associated with the remaining anatase nanoparticles at larger treatment times (observed in Figure 2), that is, larger nanoparticles with low transformation rates. It should be noted that the OA mechanism has already been observed in anatase TiO_2,[18] but this is the first time in which the growth of rutile TiO_2 nanorods has been associated with this process. Our research group observed a similar process in the growth of the SnO_2 nanocrystal rutile phase.[27]

Basically, the OA mechanism is related to the collision rate among the nanocrystals in a colloidal suspension and the reduction of surface energy, aimed at minimizing the area of high-energy faces.[16,17,27−30] Since our HRTEM results revealed the formation of nanorods with preferential growth in the [110], an analysis of the surface energy in several crystallographic

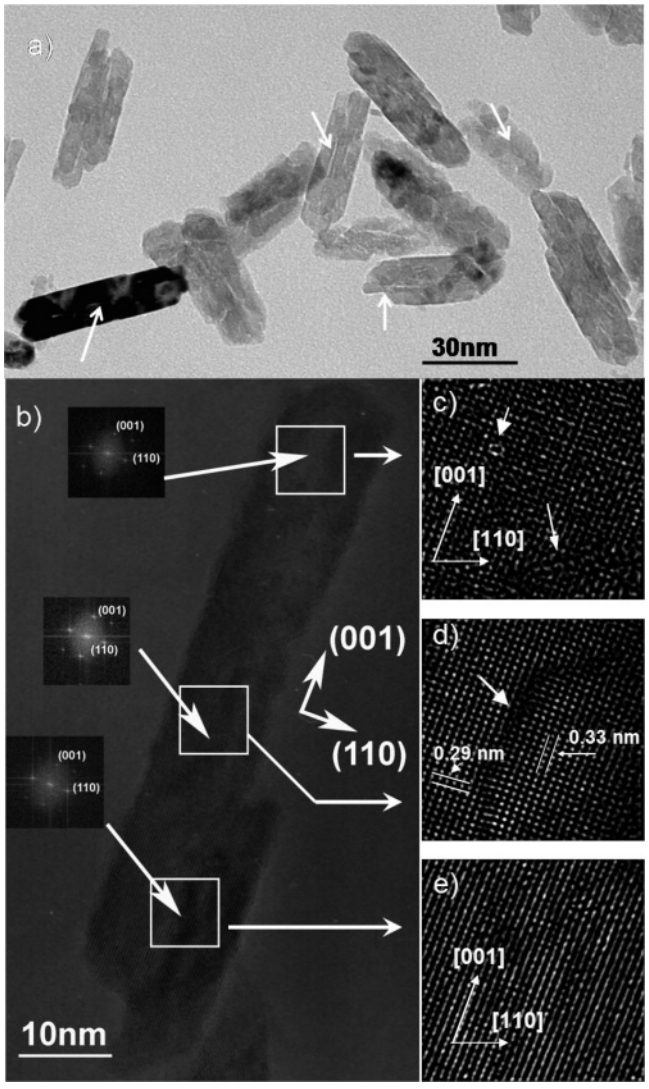

Figure 4. (a) Bright-field TEM image of R-TiO_2 nanorods showing several coalesced particles (white arrows). (b) High-magnification HRTEM image of the R-TiO_2 nanorod. The inset shows a FFT analysis of different regions in the anisotropic crystal. (c−e) Reconstructed lattice images of different areas of the nanorod shown in Figure 4a.

orientations may help us understand the growth process. The specific surface energies of rutile TiO_2 calculated from several crystalline surfaces are reported by Barnard and Zapol.[31] As expected, the (110) surface had a smaller surface energy (average surface energy of 0.37 J/m^2, based on different theoretical calculation methods) than the (001) (average surface

energy of 0.57 J/m^2, also based on different theoretical calculation methods). On the basis of this theoretical study, one can predict that anisotropic nanocrystals will be formed if the OA process occurs on high-surface-energy planes. However, crystallographically oriented growth of low-energy planes, such as that observed in the [001], is quite possible in the ϕ dimension of the nanorod. The growth in the [001] is presumably related to the collision among nanocrystals and is a strong indication that the OA process is the dominant growth mechanism due to their statistical nature.[28,32]

Summary

In summary, this article described an alternative route to process R-TiO_2 nanorods. The results presented here clearly demonstrate that the anisotropic morphology reported for R-TiO_2 nanocrystals is related to the OA process.On the basis of our XRD and STEM/HRTEM analysis, we can suppose that there is a relationship between the phase transformation and the nanocrystal growth process since the characterization of the precursor (peroxytitanate gel) by XANES demonstrated that the gel structure is not related to the final phase formation. Although this kind of relationship has already been reported in the literature, our observations of a preferential growth leads us to believe that the OA process aids phase transformation. In fact, the minimization of the area of high-energy surface faces promoted by the preferential growth process may be an extra driving force for the phase transformation from anatase TiO_2 to rutile TiO_2. On the basis of theoretical arguments, Barnard and Zapol[12] recently showed that the particle shape is a key parameter in the anatase to rutile phase transformation. This finding is congruent with our speculation. More detailed studies about this relationship are ongoing in our research group and will be the subject of a future paper.

Acknowledgment. Financial backing support by FAPESP and CNPq (both Brazilian agencies) is gratefully acknowledged. XANES measurements and HRTEM microscopy facilities were provide by LNLS, Campinas, SP, Brazil.

Note Added after ASAP Publication. This manuscript was originally published on the Web on March 29, 2007. Reference 14 has been changed. The correct version was reposted on April 5, 2007.

References and Notes

(1) Karch, J.; Birringer, R.; Gleiter, H. *Nature* **1987**, *330*, 556.
(2) Oregan, B.; Gratzel, M. *Nature* **1991**, *353*, 737.
(3) Wang, R.; Hashimoto, K.; Fujishima, A.; Chikuni, M.; Kojima, E.; Kitamura, A.; Shimohigoshi, M.; Watanabe, T. *Nature* **1997**, *388*, 431.
(4) Kavan, L.; Gratzel, M.; Rathousky, J.; Zukal, A. *J. Electrochem. Soc.* **1996**, *143*, 394.
(5) Jiang, X. C.; Herricks, T.; Xia, Y. N. *Adv. Mater.* **2003**, 15, 1205.
(6) Han, S.; Choi, S. H.; Kim, S. S.; Cho, M.; Jang, B.; Kim, D. Y.; Yoon, J.; Hyeon, T. *Small* **2005**, *1*, 812.
(7) Zhang, H. Z.; Finnegan, M.; Banfield, J. F. *Nano Lett.* **2001**, *1*, 81.
(8) Niederberger, M.; Bartl, M. H.; Stucky, G. D. *Chem. Mater.* **2002**, *14*, 4364.
(9) Polleux, J.; Pinna, N.; Antonietti, M.; Niederberger, M. *Adv. Mater.* **2004**, *16*, 436.
(10) Zhang, H. Z.; Banfield, J. F. *J. Mater. Chem.* **1998**, *8*, 2073.
(11) Zhang, H. Z.; Banfield, J. F. *J. Phys. Chem. B* **2000**, *104*, 3481.
(12) Barnard, A. S.; Zapol, P. *J. Phys. Chem. B* **2004**, *108*, 18435.
(13) Wang, W.; Gu, B. H.; Liang, L. Y.; Hamilton, W. A.; Wesolowski, D. J. *J. Phys. Chem. B* **2004**, *108*, 14789.
(14) Zhang, Q.; Gao, L. *Langmuir* **2003**, *19*, 967.
(15) Wu, M. M.; Lin, G.; Chen, D. H.; Wang, G. G.; He, D.; Feng, S. H.; Xu, R. R. *Chem. Mater.* **2002**, *14*, 1974.
(16) Penn, R. L.; Banfield, J. F. *Am. Mineral.* **1998**, *83*, 1077.
(17) Penn, R. L.; Banfield, J. F. *Science* **1998**, *281*, 969.
(18) Penn, R. L.; Banfield, J. F. *Geochim. Cosmochim. Acta* **1999**, *63*, 1549.
(19) Mühlebach, J.; Müller, K.; Schwarzenbach, G. *Inorg. Chem.* **1970**, *9*, 2381.
(20) Schwarzenbach, D. *Inorg. Chem.* **1970**, *9*, 2391.
(21) Chen, L. X.; Rajh, T.; Wang, Z. Y.; Thurnauer, M. C. *J. Phys. Chem. B* **1997**, *101*, 10688.
(22) Luca, V.; Djajanti, S.; Howe, R. F. *J. Phys. Chem. B* **1998**, *102*, 10650.
(23) Hanley, T. L.; Luca, V.; Pickering, I.; Howe, R. F. *J. Phys. Chem. B* **2002**, *106*, 1153.
(24) Sergienko, V. S. *Crystallogr. Rep.* **2004**, *49*, 907.
(25) Navrotsky, A. *Proc. Natl. Acad. Sci. U.S.A.* **2004**, *101*, 12096.
(26) Gribb, A. A.; Banfield, J. F. *Am. Mineral.* **1997**, *82*, 717.
(27) Leite, E. R.; Giraldi, T. R.; Pontes, F. M.; Longo, E.; Beltran, A.; Andres, J. *Appl. Phys. Lett.* **2003**, *83*, 1566.
(28) Ribeiro, C.; Lee, E. J. H.; Longo, E.; Leite, E. R. *ChemPhysChem* **2005**, *6*, 690.
(29) Ribeiro, C.; Lee, E. J. H.; Longo, E.; Leite, E. R. *ChemPhysChem* **2006**, *7*, 664.
(30) Zhang, H. Z.; Banfield, J. F. *Am. Mineral.* **1999**, *84*, 528.
(31) Barnard, A. S.; Zapol, P. *Phys. Rev. B* **2004**, *70*, 235403.
(32) Ribeiro, C.; Lee, E. J. H.; Giraldi, T. R.; Varela, J. A.; Longo, E.; Leite, E. R. *J. Phys. Chem. B* **2004**, *108*, 15612.